Paracrystalline Lattice Distortion in Crystalline Pharmaceuticals Determination of Paracrystalline Lattice Distortion by Powder X-Ray Diffraction

Eihei FUKUOKA,* Katsuhide TERADA,[1] Midori MAKITA, and Shigeo YAMAMURA

School of Pharmaceutical Sciences, Toho University, 2–2–1 Miyama, Funabashi, Chiba 274, Japan.
Received November 17, 1994; accepted December 30, 1994

The lattice distortion and size of crystallites along a particular lattice direction in solid pharmaceuticals were determined by profile analysis using a peak profile of X-ray powder diffraction. The analysis was carried out according to either the paracrystal or micro strain model. After correction for instrumental broadening, pure diffraction profiles of several orders of $0k0$ reflections for dibasic calcium phosphate dihydrate (DCPD) and those of $0kk$ reflections for griseofulvin (GRIS) were obtained. Then, the integral breadths of the pure diffraction profiles were calculated. Lattice distortion and the size of crystallites along [$0k0$] of DCPD and those along [$0kk$] of GRIS were determined from the slope and ordinate intercept of the straight line obtained by plotting the integral breadth against the order of reflection according to the theory of paracrystalline diffraction. DCPD powders were characterized to have paracrystalline lattice distortion, in which broadening profiles of both the size of crystallites and lattice distortion are of a Gaussian shape. The lattice distortion along [$0k0$] increased, while the size of crystallites scarcely decreased with the progress of grinding time. GRIS powders were characterized to have paracrystalline lattice distortion, in which both broadening profiles of the size of crystallites and lattice distortion, are of a Cauchy (Lorentzian) shape. The lattice distortion along [$0kk$] increased and the size of crystallites decreased with the progress of grinding time. The effects of lattice distortion on physicochemical and pharmaceutical properties of DCPD and GRIS powders were discussed.

Key words paracrystal; lattice distortion; X-ray powder diffraction; crystallinity; crystallite size

There are several reports which have analyzed the degree of crystallinity of solid pharmaceuticals,[2] because the degree of crystallinity may affect the stability and bioavailability of drugs.[3] Solid pharmaceuticals may have some kind of distortion or disorder in their crystal lattice, and there are some reports which assess the degree of disorder by means of microcalorimetry and X-ray diffractometry.[4] It is important to evaluate the lattice distortion quantitatively, because lattice distortion may play an important role in the pharmaceutical properties of solid drugs.

In the present paper, we report the profile analysis method for evaluating the lattice distortion and size of crystallites using X-ray powder diffraction data. The purpose of the present work is to determine the lattice distortion along a particular lattice direction in solid pharmaceuticals and to reveal the change in lattice distortion as the result of grinding. Furthermore, the effects of lattice distortion on physicochemical and pharmaceutical properties of drugs were discussed.

Theoretical

Paracrystal Model Hosemann postulated that a real crystal structure has two kinds of distortions.[5] In a distortion of the first kind, the long range order is preserved, and the effect of first kind distortion is indistinguishable from that of thermal motions. On the other hand, in a lattice possessing distortion of the second kind, the long range order is lost whereas the short range order of lattice points is present. Substances having distortion of second kind are called paracrystal. Distortions of the second kind result in a diminution of intensity and an increase in reflection breadth with increases in the 2θ or order of reflection (m). In the theory of paracrystalline diffraction, observed diffraction profiles are influenced not only by the size of crystallites but also by the lattice distortion. If both broadening profiles of the size of crystallites and lattice distortion are of Gaussian shape, pure reflection breadth in s ($=2\sin\theta/\lambda$) scale, $(\delta_s)_o$, increased with an increase in m, as in Eq. 1.[6]

$$(\delta_s)_o^2=(\delta_s)_c^2+(\delta_s)_{II}^2=1/L_{hkl}^2+(\pi g_{II})^4 m^4/d_{hkl}^2 \quad (1)$$

where $(\delta_s)_o$ is the pure reflection breadth free of instrumental broadening, $(\delta_s)_c$ is the broadening profile of the size of crystallites, $(\delta_s)_{II}$ is the broadening profile of the lattice distortion of the second kind, L_{hkl} is the size of crystallites along [hkl], g_{II} is the paracrystalline lattice distortion parameter (relative distance fluctuation, $\Delta d_{hkl}/d_{hkl}$), m is the order of reflection, and d_{hkl} is the interplanar distance of the (hkl) plane. This equation is valid if lattice distortion ($2\pi^2 g_{II}^2 m^2$) is much smaller than unity and the profiles of $(\delta_s)_c$ and $(\delta_s)_{II}$ are of a Gaussian shape.[6] After correction for instrumental broadening, the squared integral breadths of the pure diffraction profiles are plotted against m^4, which yields a straight line with an ordinate intercept $1/L_{hkl}^2$ and slope $(\pi g_{II})^4/d_{hkl}^2$, permitting L_{hkl} and g_{II} to be determined.

If the broadening profiles are of Cauchy (Lorentzian) shape, Eq. 1 should be replaced by Eq. 2.[7]

$$(\delta_s)_o=(\delta_s)_c+(\delta_s)_{II}=1/L_{hkl}+(\pi g_{II})^2 m^2/d_{hkl} \quad (2)$$

On the basis of the Cauchy assumption, g_{II} and L_{hkl} were determined from the slope and ordinate intercept of the straight line which plotted $(\delta_s)_o$ against m^2.

Micro Strain Model Warren and Averbach have reported a method of integral breadths by which they de-

* To whom correspondence should be addressed.

termined the size of crystallites and local lattice distortion (micro strain).[8] When the peak profiles broaden by not only the size of crystallites but also lattice distortion, the actual broadening effect would depend on the shapes of the two contribution profiles. These are commonly assumed to be either Gaussian or Cauchy (Lorentzian), as Eqs. 3 and 4.

$$(\delta_s)_o^2=(\delta_s)_c^2+(\delta_s)_D^2=1/L_{hkl}^2+(2es)^2 \quad \text{(Gaussian)} \tag{3}$$

$$(\delta_s)_o=(\delta_s)_c+(\delta_s)_D=1/L_{hkl}+(2es) \quad \text{(Cauchy)} \tag{4}$$

where $(\delta_s)_D$ is the broadening profile of lattice distortion, e is vaguely defined as the upper limit of the lattice distortions[8] and s is the magnitude of the reciprocal lattice vector of the hkl reflections. On the basis of Gaussian assumption, e and L_{hkl} were calculated from the slope and ordinate intercept of the straight line which plotted $(\delta_s)_o^2$ against s^2. In Cauchy assumption, they were obtained from the straight line which plotted $(\delta_s)_o$ against s.

When the peak profiles from at least three well-resolved orders of hkl reflection were obtained, the model of lattice distortion (paracrystalline or micro strain) should be estimated from the linearity of the relations of $(\delta_s)_o$ and m or s, plotted according to Eqs. 1 to 4. The lattice distortion and L_{hkl} can be determined from the slope and ordinate intercept of the straight line.

Experimental

Materials Dibasic calcium phosphate dihydrate (DCPD, Yoshida Pharmaceutical Co.) was of JP grade and used without further purification. Griseofulvin (GRIS, Nihon Kayaku Co.) was of JP grade and used after recrystallization from acetone. Ground samples were prepared using a ball mill made of tungsten-carbide. A grinding apparatus (P-6, Fritsch Co.) was used for grinding. Intact and ground powders were used after being passed through a 250 mesh sieve. Crystal structures of DCPD and GRIS have been determined previously.[9,10]

X-Ray Diffraction A RAD type diffractometer (Rigaku Denki Co.) was used. An X-ray source was β-filtered Cu-K_α line. Diffraction intensities were measured by a fixed-time step-scanning method described previously.[11] Observed peak profiles were approximated by the modified Lorentzian function,[12] and the desecrate Bragg reflections were separated from background scattering by a non-linear least-squares procedure.

1) Correction for Instrumental Broadening: Instrumental broadening based on the slit widths in a goniometer was corrected by Eagun's successive convolution method.[13] The profiles of 100 reflections from a (100)-faced aspirin crystal, cut out to exhibit 25 × 15 mm of the (100)-face from a well grown large crystal, and that of 111 reflections of silicon powder were used as standard profiles (instrumental broadening profile), being free of the broadenings of the size of crystallites and lattice distortion. The former was used for the profiles of 020 and 040 reflections in DCPD, and those of 011 and 022 reflections in GRIS. The latter was used for the profile of 060 reflection in DCPD and that of 033 reflection in GRIS. The effect of diffraction of the $K_{\alpha 2}$ line is removed with the correction of instrumental broadening. After this correction, integral breadths of the pure diffraction profiles were calculated.

2) Degree of Crystallinity: The degree of crystallinity and lattice disorder parameter were determined by the Ruland method.[14]

Specific Surface Area The specific surface area of the sample powder was determined by the BET method[15] from a nitrogen gas adsorption isotherm at liquid nitrogen temperature using Accusorb 2100E (Shimadzu).

Rate of Water Penetration The rate of water penetration into DCPD powder beds was measured by the powder method.[16]

Dissolution Test The dissolution behavior of GRIS was measured by the rotating disk method with 200 ml of 0.02 M phosphate buffer (pH 7.2) maintained at 35 °C. Disks (6.5 mm in diameter) were prepared by the compression under 400 kg/cm^2 and rotated at 100 rpm. The dissolution medium was circulated between the dissolution vessel and a flow cell made of quarts by a peristaltic pump. The absorbance at 290 nm was recorded continuously by a UV spectrophotometer.

Results and Discussion

Analysis of Lattice Distortions and Size of Crystallites DCPD: Figure 1 shows the X-ray powder diffraction patterns of intact and ground DCPD powders. Because the diffraction lines of some orders of $0k0$ reflections, 020, 040 and 060 reflections, were observed without mutual overlap with other diffraction lines, DCPD was available for the present analysis. Figure 2 shows the observed and simulation profiles of 020, 040 and 060 reflections. After the subtraction of background intensities, the peak profiles were corrected for instrumental broadening by using the Eagun's method.[13] The integral breadths of pure diffraction profiles being free of instrumental broadening were calculated and plotted according to either the paracrystal or micro strain model (Fig. 3). The experimental data did not sufficiently characterize the model of distortion in intact DCPD powder. In the ground samples, the best linear relationships were observed in the case of the plots of squared integral breadths against m^4 (Fig.

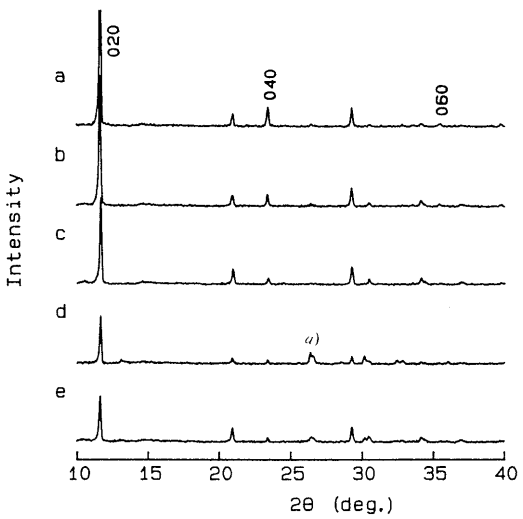

Fig. 1. X-Ray Diffraction Patterns of Intact and Ground DCPD Powders

a) Intact powder; b) ground for 3 h; c) ground for 7 h; d) ground for 10 h; e) ground for 15 h. *a)* Indicates the diffraction peak for dibasic calcium phosphate anhydride.

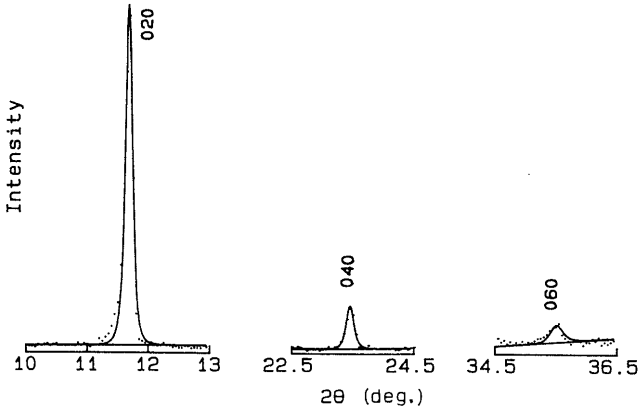

Fig. 2. Observed Diffraction Intensities and Simulated Pattern of 020, 040 and 060 Reflections of DCPD

Dots are observed intensities. Solid lines are simulated peak profiles.

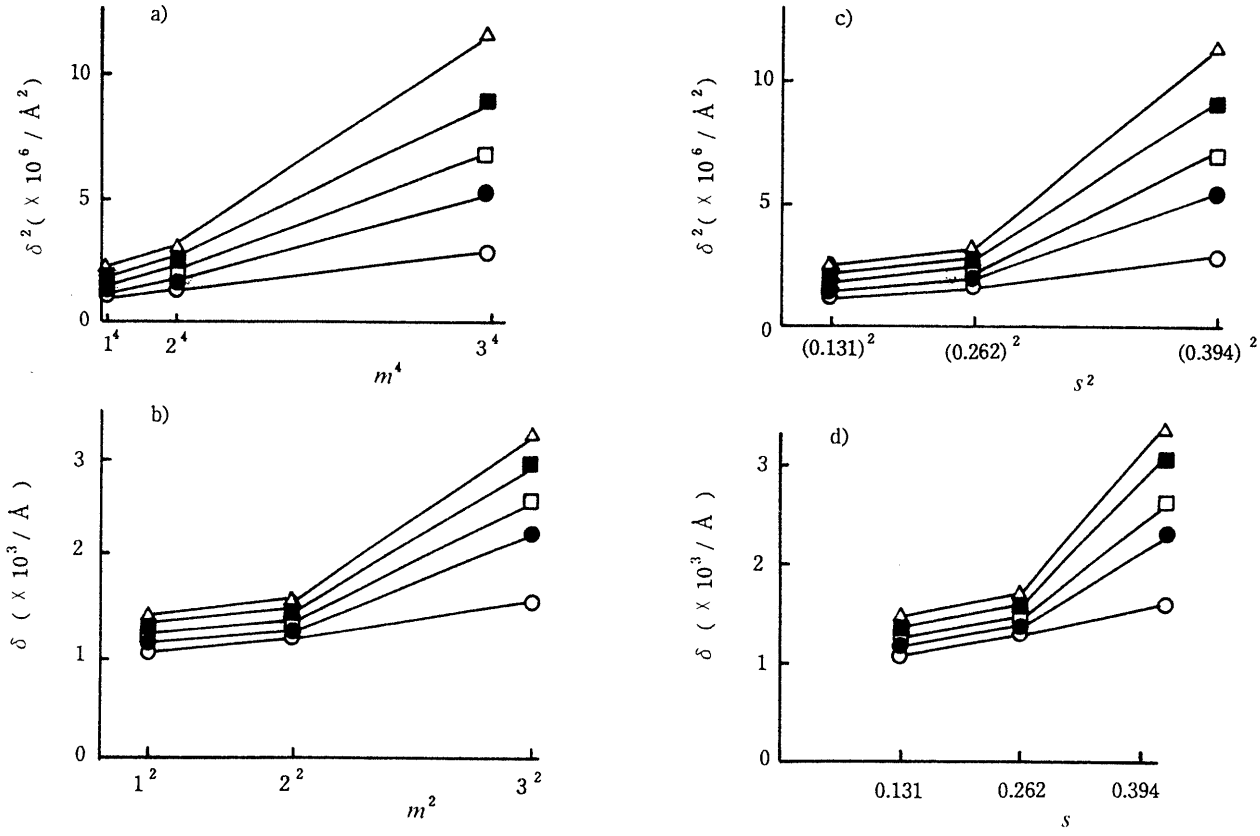

Fig. 3. Plots of Integral Breadths against s or m for DCPD

a) Plot according to the paracrystal model assuming Gaussian broadening profiles; b) plot according to the paracrystal model assuming Cauchy broadening profiles; c) plot according to the micro strain model assuming Gaussian broadening profiles; d) plot according to the micro strain model assuming Cauchy broadening profiles. ○, intact powder; ●, ground for 3 h; □, ground for 7 h; ■, ground for 10 h; △, ground for 15 h.

Table 1. Lattice Distortion (Relative Distance Fluctuation) and Size of Crystallites of DCPD Calculated by Paracrystal Model

Sample	Lattice distortion (%)	Size of crystallites (Å)
Intact powder	0.89	879
Ground for 3 h	0.98	808
Ground for 7 h	1.35	810
Ground for 10 h	1.48	817
Ground for 15 h	1.55	807

3a). Thus DCPD powders were considered to have a paracrystalline lattice distortion with Gaussian broadening profiles of the size of crystallites and lattice distortion. The paracrystalline lattice distortion parameter (relative distance fluctuation: g_{II}) and size of crystallites of DCPD powders calculated from Eq. 1 are summarized in Table 1. Although the size of crystallites remained almost constant, the lattice distortion along [0k0] increased with the progress of grinding time.

GRIS: Figure 4 shows the X-ray diffraction patterns of intact and ground GRIS powders. The profiles of 011, 022 and 033 reflections were observed without mutual overlap with other reflections. Figure 5 shows the observed and simulation profiles of the 011, 022 and 033 reflections. After subtraction of background intensities and correction for the instrumental broadening, the integral breadths were plotted according to either the paracrystal or micro strain model (Fig. 6). On the whole, the best linear relationships

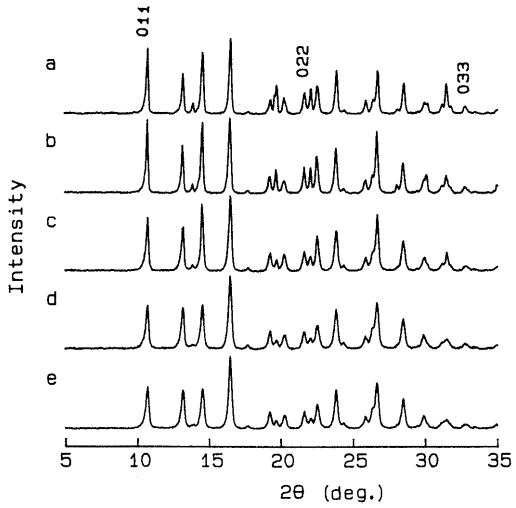

Fig. 4. X-Ray Diffraction Patterns of Intact and Ground GRIS Powders

a) Intact powder; b) ground for 1 h; c) ground for 3 h; d) ground for 5 h; e) ground for 7 h.

were observed in the case of the plots of the integral breadths against m^2 (Fig. 6b). Thus, GRIS powders were reasonably considered to have a paracrystalline lattice distortion with Cauchy broadening profiles corresponding to the size of crystallites and lattice distortion. Changes in the size of crystallites and lattice disorder parameters, along [0kk] with the progress of grinding time, are sum-

marized in Table 2. Lattice distortion increased and the size of crystallites of GRIS decreased as grinding time progressed. Thus, grinding was effective not only in increasing the lattice distortion but also in decreasing the size of crystallites in GRIS.

Change in Crystallinity and Specific Surface Area of DCPD and GRIS by Grinding DCPD: The degree of crystallinity determined by the Ruland method and the specific surface area determined by the nitrogen gas adsorption method of intact and ground DCPD are summarized in Table 3. As described before, the lattice distortion along [0k0] determined by the profile analysis increased with the progress of grinding time, however the degree of crystallinity (X_{cr}) and lattice disorder parameter (k) showed little change. This result suggests that a small change in lattice distortion along the particular lattice direction had little influence on the X_{cr} and k determined by the Ruland method. Because the Ruland method presupposes the random orientation of crystallites in the specimen, a lattice distortion along the particular lattice direction may have little effect on X_{cr} and k. Thus the

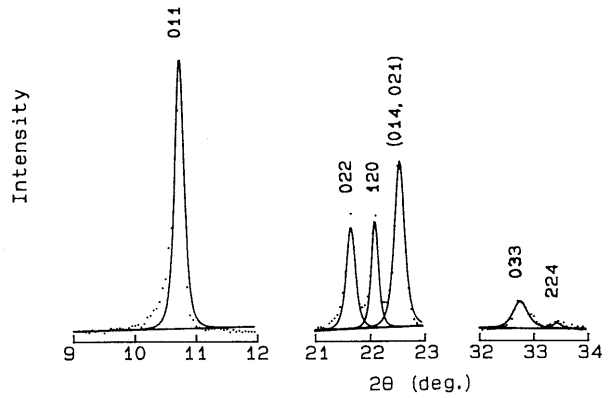

Fig. 5. Observed Diffraction Intensities and Simulated Pattern of 011, 022 and 033 Reflections of GRIS

Dots are observed intensities. Solid lines are simulated peak profiles.

Table 2. Lattice Distortion (Relative Distance Fluctuation) and Size of Crystallites of GRIS Calculated by Paracrystal Model

Sample	Lattice distortion (%)	Size of crystallites (Å)
Intact powder	0.98	613
Ground for 1 h	1.15	568
Ground for 3 h	1.41	426
Ground for 5 h	1.45	393
Ground for 7 h	1.54	382

Table 3. Degree of Crystallinity and Specific Surface Area of DCPD

Sample	X_{cr} (%)[a]	k (Å^2)[a]	S_w (m^2/g)[b]
Intact powder	72	0.8	1.4
Ground for 3 h	74	0.7	1.8
Ground for 7 h	69	0.7	2.0
Ground for 10 h	71	0.9	2.5
Ground for 15 h	69	0.8	3.2

a) Degree of crystallinity (X_{cr}) and disorder parameter (k) were determined by the Ruland method. *b*) Specific surface area (S_w) was determined by the BET method.

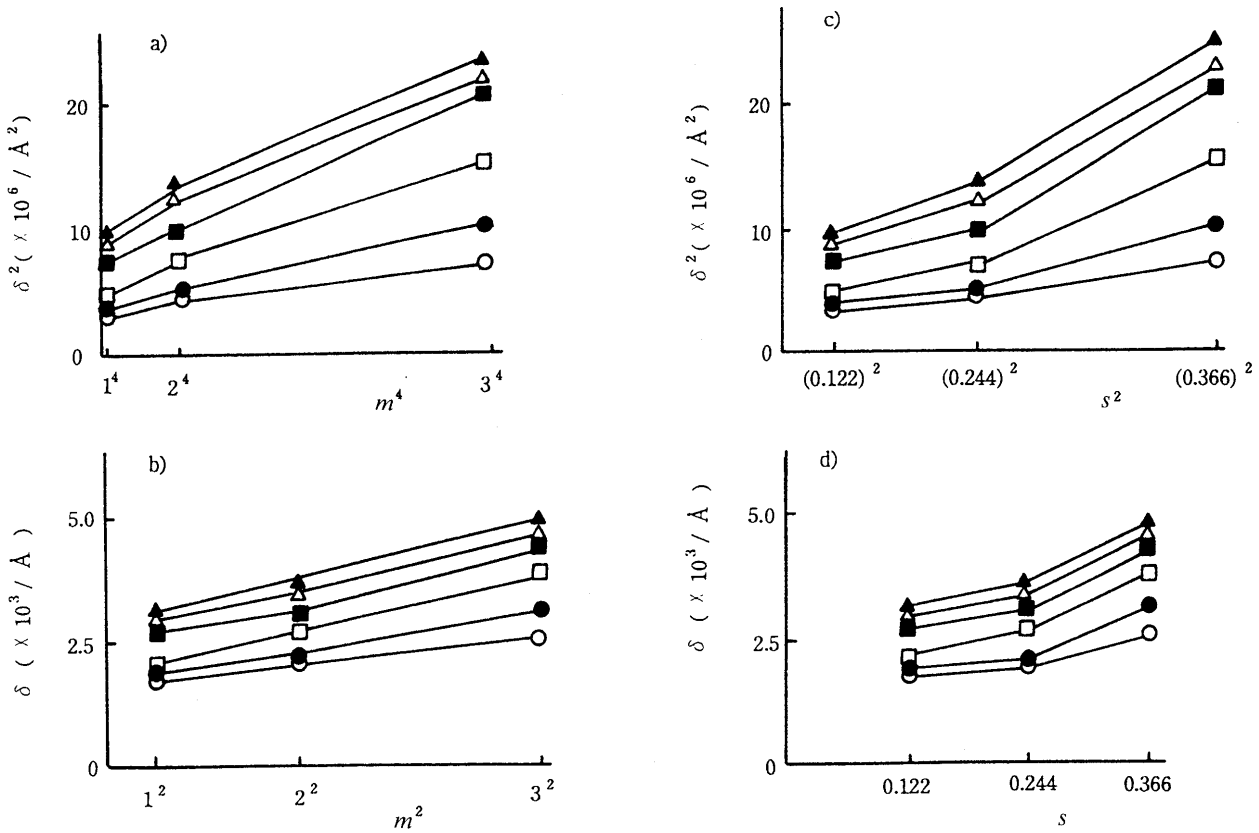

Fig. 6. Plots of Integral Breadths against s or m for GRIS

a) Plot according to the paracrystal model assuming Gaussian broadening profiles; b) plot according to the paracrystal model assuming Cauchy broadening profiles; c) plot according to the micro strain model assuming Gaussian broadening profiles; d) plot according to the micro strain model assuming Cauchy broadening profiles. ○, intact powder; ●, ground for 1 h; □, ground for 3 h; ■, ground for 5 h; △, ground for 7 h.

Table 4. Degree of Crystallinity and Specific Surface Area of GRIS

Sample	X_{cr} (%)[a]	k (Å^2)[a]	S_w (m^2/g)[b]
Intact powder	75	2.4	0.3
Ground for 1 h	71	2.9	2.1
Ground for 3 h	67	2.8	3.3
Ground for 5 h	67	3.1	3.5
Ground for 7 h	64	3.0	3.9

a) Degree of crystallinity (X_{cr}) and disorder parameter (k) were determined by the Ruland method. *b*) Specific surface area (S_w) was determined by the BET method.

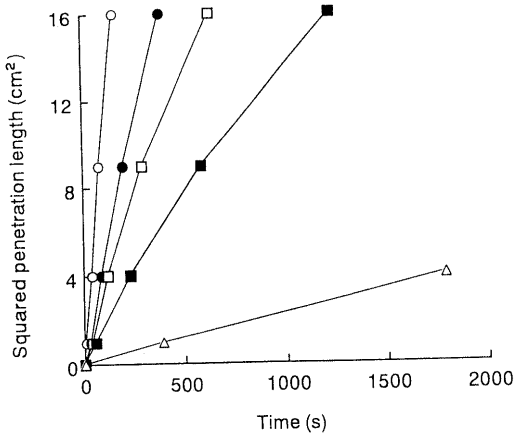

Fig. 7. Rate of Water Penetration into Intact and Ground DCPD Powder Beds

○, intact powder; ●, ground for 3 h; □, ground for 7 h; ■, ground for 10 h; △, ground for 15 h. Each point represents the mean of three experiments.

profile analysis method would have a higher sensitivity to detect the lattice distortions rather than the Ruland method.

The specific surface area (S_w) of DCPD powders increased gradually from 1.4 to 3.2 m^2/g with the progress of grinding time.

GRIS: The X_{cr}, k and S_w of intact and ground GRIS are summarized in Table 4. X_{cr} decreased, k slightly increased and S_w increased gradually from 0.3 to 3.9 m^2/g with the progress of grinding time. In the GRIS powders, a decrease in X_{cr} and increase in k correlated with the increase in lattice distortion along [0kk].

The profile analysis method does not provide information about the degree of crystallinity; this method, however, had a higher sensitivity for determination of the lattice distortion along a particular lattice direction. An increase in S_w may correlate with a decrease in the size of crystallites determined by the profile analysis.

Influence of Lattice Distortion on Some Pharmaceutical Properties of DCPD and GRIS DCPD: Figure 7 shows the rate of water penetration into DCPD powder beds by plotting the squared penetration length against time, according to Washburn's equation.[17] The rate of water penetration into DCPD powder beds decreased with the progress of grinding time. As shown in Fig. 1, after being ground for 10 h, the diffraction peak of dibasic calcium phosphate anhydride appeared, and wettability became extremely poor. The contact angle between dibasic calcium phosphate anhydride and water was considered to be larger than that between DCPD and water. Although the increase

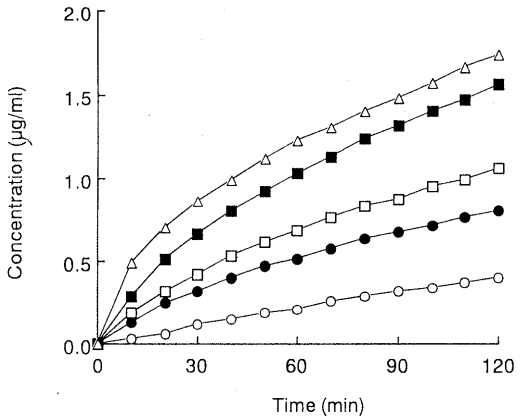

Fig. 8. Dissolution Behavior of Intact and Ground GRIS

○, intact powder; ●, ground for 1 h; □, ground for 3 h; ■, ground for 5 h; △, ground for 7 h.

in S_w was small up to 7 h of grinding time (Table 3), the rate of water penetration obviously decreased, indicating that the change in surface properties of DCPD particles retarded the water penetration. Small lattice distortion produced by grinding may change the surface properties of DCPD particles. Recently, Landen *et al.*, reported that DCPD powder had intermanufacturer variability and the particle size of DCPD had a strong influence on their dehydration behavior.[18] Some pharmaceutical properties of DCPD would be influenced not only by particle size but also by lattice distortion along [0k0].

GRIS: Figure 8 shows the dissolution behaviors of intact and ground GRIS in a phosphate buffer. The dissolution rate of GRIS increased with a longer grinding time. According to Ostwald and Freundlich's equation,[19] the reduction of particle size results in the increase in solubility, per Eq. 5.

$$\boldsymbol{RT}/M \ln(S_2/S_1) = 4\gamma/\rho(1/d_1 - 1/d_2) \quad (5)$$

where $\boldsymbol{R}$ is the gas constant, T is the absolute temperature, M is the molecular weight, S_1 and S_2 are the solubilities of the particles with diameter d_1 and d_2, γ is the surface energy, and ρ is the true density of the particles. Assuming spherical particles, it is possible to calculate the mean particle size (d_m) by Eq. 6.

$$d_m = 6/(\rho S_w) \quad (6)$$

When ρ of GRIS was postulated to be 1.54 g/cm^3,[10] the d_m of GRIS powders before grinding and after being ground for 7 h was calculated to be 13.5 and 1.1 μm from S_w (Table 4), respectively. When these values were substituted in Eq. 5, the increase in solubility of GRIS with a reduction in particle size would be expected to be less than 1%. Therefore, the increase in the rate of dissolution would not be caused by the increase in solubility accompanied by the reduction of particle size. Because the dissolution studies were carried out under the condition of constant surface area (the rotating disk method), changes in the specific surface area would not influence the dissolution rate. Moreover, the decrease in crystallinity of GRIS by grinding was not a significant amount. So, an increase in the dissolution rate of GRIS might be affected by an increased in lattice distortion.

It is known that a decrease in particle size results in an increase in the bioavailability of GRIS.[20] The mechanism was reported as the result of the dissolution rate increasing with an increase in the surface area by a reduction of particle size. The results presented here suggest that the dissolution and subsequent absorption of poorly water-soluble drugs may be dependent not only on the particle size but also on the lattice distortion.

In conclusion, the profile analysis method was presented for determining the size of crystallites and lattice distortion along a particular lattice direction. In the present method, it is necessary to produce at least three well-resolved profiles for the analysis of the model of distortion and lattice distortion. Because of this limitation, this method is not always suitable for analyzing the lattice distortion of crystalline pharmaceuticals. This profile analysis method had higher sensitivity for detecting lattice distortion along the particular lattice direction rather than the Ruland method. Crystalline powders of DCPD and GRIS were characterized as having some paracrystalline lattice distortion and the lattice distortion was increased by grinding. Some pharmaceutical properties of crystalline drugs might be affected by lattice distortion along the particular lattice direction. We hope to report on another method that has wider applicability for the analysis of lattice distortion in crystalline pharmaceuticals.

References and Notes

1) Present address: *Chugai Pharmaceutical Co., Ltd., 41–8, Takada 3-chome, Toshima-ku, Tokyo 171, Japan.*
2) Nakai Y., Fukuoka E., Nakajima S., Morita M., *Chem. Pharm. Bull.*, **30**, 1811 (1982); Fukuoka E., Makita M., Yamamura S., *ibid.*, **41**, 595 (1993).
3) Morita M., Hirota S., Kikuno K., Kataoka K., *Chem. Pharm. Bull.*, **33**, 795 (1985); Oguchi T., Terada K., Yamamoto K., Nakai Y., *ibid.*, **37**, 1881 (1989).
4) S-Gerhardt A., Ahleneck C., Zografi G., *Int. J. Pharmaceut.*, **104**, 237 (1994); Sebhatu T., Angberg M., Ahlneck C., *ibid.*, **104**, 135 (1994).
5) Hosemann R., Baguchi S. N., "Direct Analysis of Diffraction by Matter," North-Holland Publishing Co., Amsterdam, 1962.
6) Bonart R., Hosemann R., McCullouch R. L., *Polymer*, **4**, 199 (1963); Hosemann R., Wilke W., *Faserforsch. Textiltechnik*, **15**, 521 (1964).
7) Hosemann R., Wilke W., *Macromol. Chem.*, **118**, 230 (1968).
8) Warren B. E., Averbach B. L., *J. Appl. Phys.*, **21**, 595 (1950); Buchanan D. R., Miller R. L., *ibid.*, **37**, 4003 (1966).
9) Jones D. W., Smith J. A. S., *J. Chem. Soc.*, **1962**, 1414.
10) Malmros G., Wagner A., Maron L., *Cryst. Struct. Commun.*, **6**, 463 (1977).
11) Fukuoka E., Makita M., Yamamura S., *Chem. Pharm. Bull.*, **39**, 3313 (1991).
12) Sonnevert E. J., Visser J. W., *J. Appl. Crystallogr.*, **8**, 1 (1977).
13) Ergun S., *J. Appl. Crystallogr.*, **1**, 19 (1968).
14) Ruland W., *Acta Cryst.*, **14**, 1180 (1961).
15) Brunauer S., Emmett P. H., Teller E., *J. Am. Chem. Soc.*, **60**, 309 (1938).
16) Fukuoka E., Kimura S., Makita M., *Chem. Pharm. Bull.*, **29**, 295 (1981).
17) Washburn E. H., *Phys. Rev.*, **17**, 273 (1921).
18) Landin M., M-Pacheco R., G-Amoza J. L., Souto C., Concheiro A., Rowe R. C., *Int. J. Pharmaceut.*, **103**, 9 (1994); Landin M., Rowe R. C., York P., *ibid.*, **104**, 271 (1994).
19) Ostawald W., *Zeitschr. Physik. Chem.*, **34**, 495 (1900); Gennaro A. R. (ed.), "Remington's Pharmaceutical Sciences," 18th ed., Mack Publishing Co., Pennylvania, 1990, p. 591.
20) Atkinson R. M., Bedford C., Child K. J., Tomich E. G., *Antibiot. Chemother.*, **12**, 232 (1962).